EVALUATING RADIATION DAMPING OF SHALLOW FOUNDATIONS ON NONLINEAR SOIL MEDIUM FOR SOIL-STRUCTURE INTERACTION ANALYSIS OF BRIDGES

Jian Zhang[1] and Yuchuan Tang[2]

Abstract

The paper evaluates the radiation damping associated with shallow foundations sitting on linear or nonlinear soil medium. The study is motivated by the need to develop a macroscopic foundation model that can realistically capture the nonlinear behavior and energy dissipation mechanism of shallow foundations. Such model is essential to simulate the complex behavior of bridges sitting on flexible foundations due to soil-structure interaction effects. In this study, the dynamic response of an infinitely long strip foundation resting on an elastic and inelastic half-space is investigated. The study revealed responses' strong dependency on amplitude and frequency of the motion. It also found that the radiation damping of nonlinear soil medium is significantly lower than the elastic soil counterpart, which in turn affects the bridge response.

Introduction

Recent earthquakes in major urban areas have underscored the need to better understand the responses of bridges to seismic actions. The responses of bridges are affected by not only the nonlinear dynamic behavior of individual components (i.e. superstructure, foundations and surrounding soil) but also the complex interaction among them, i.e. the soil-structure interaction effects. In particular, the changing stiffness and energy dissipation either by means of hysteretic damping or radiation damping are the most important characteristics of soil-structure interaction. In this study, the radiation damping and its effects are evaluated for bridges sitting on shallow foundations. Although various models are available to account for radiation damping of shallow foundations on elastic soil medium (Veletsos and Verbic 1974; Luco and Westmann 1972; Hryniewicz 1981; Gazetas 1991 and Veletsos et al. 1997 among others), there are essentially no previous studies on evaluating the radiation damping of shallow foundations on nonlinear soil medium.

In this study, finite element method is adopted to compute the dynamic response of an infinitely long strip foundation resting on an elastic and inelastic half-space. Numerical results from finite element method are compared with theoretical solution of strip foundation resting on elastic half-space so as to provide guidance on choosing appropriate domain scale, mesh size and boundaries for subsequent nonlinear analysis. Closed-form formulas are developed to describe the linear frequency-dependent dynamic stiffness. The study utilizes realistic nonlinear constitutive models to exhibit yielding and kinematic hardening behavior of soil. An extensive parametric study has been conducted

[1] Assistant Professor, Dept. of Civil and Environmental Engr., Univ. of California, L.A.
[2] Graduate Researcher, Dept. of Civil and Environmental Engr., Univ. of California, L.A.

to reveal the amplitude and frequency dependent response of strip foundation. In particular, the radiation damping is evaluated when there is yielding in soil medium.

Dynamic Stiffness of Rigid Strip Foundation on Elastic Soil Half-space

Consider an infinitely-long rigid strip foundation sitting on elastic half-space, as shown in Figure 1. Its dynamic stiffness can be obtained analytically. Muskhelishvili (1963) first conducted the static analysis and revealed the zero stiffness of strip foundation in either vertical or horizontal direction. Luco and Westmann (1972) later derived theoretic dynamic compliance of rigid strip foundation bonded to an elastic soil half-space using the theory of singular integral equations. An exact solution was presented for incompressible soil (Poisson's ratios ν=0.5) while approximate solutions were obtained for soil of Poisson's ratio ν=0, 1/4, and 1/3.

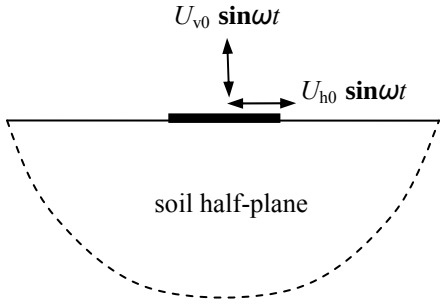

Fig. 1 Foundation geometry and excitation conditions

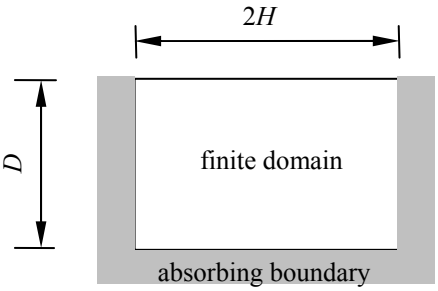

Fig. 2 Finite domain and absorbing boundary

Hryniewicz (1981) obtained the dynamic stiffness of rigid strip foundation on an elastic half-space of Poisson's ratio ν=0.25. Under a harmonic motion, the reacting forces are related to displacements by the general form shown in Eq. (1):

$$\begin{Bmatrix} P_v(t) \\ P_h(t) \end{Bmatrix} = \pi G \begin{bmatrix} c_{11} + \mathrm{i}d_{11} & 0 \\ 0 & c_{22} + \mathrm{i}d_{22} \end{bmatrix} \begin{Bmatrix} U_v(t) \\ U_h(t) \end{Bmatrix} \tag{1}$$

where G is the shear modulus of soil, $\pi G(c_{11}+\mathrm{i}d_{11})$ and $\pi G(c_{22}+\mathrm{i}d_{22})$ is the dynamic stiffness in vertical and horizontal directions respectively. The force-displacement relationship in Eq. (1) is analogous to that of a spring-dashpot system with spring constant $\pi G c_{\mathrm{ii}}$ and dashpot coefficient $\pi G d_{\mathrm{ii}}/\omega$, i =1 or 2. The dynamic stiffness parameters c_{11}, d_{11}, c_{22}, d_{22} depend on both displacement excitation frequency and soil properties. The dynamic stiffness parameters are conventionally plotted versus dimensionless frequency $a_0= \omega b/v_s$ for a given Poisson's ratio, where b is the half-width of strip foundation and v_s is the shear wave velocity in soil medium.

Finite element method is used in this study to conduct the dynamic analyses of strip foundation under harmonic displacement excitation in vertical and horizontal directions respectively. The soil half-space is represented with a finite domain where an absorbing boundary condition needs to be present to correctly model the outgoing waves of an infinite domain (Fig. 2). Maximum element size, boundary condition and scale of the finite domain dominate the accuracy of finite element analysis results of dynamic response of strip foundation. Judicious selection of domain scale and mesh size is required to minimize the numerical oscillations that were often observed with finite element method.

The maximum element size is controlled by the shear wave length L. Kuhlemeyer and Lysmer (1973) and Lysmer et al. (1975) suggested that the maximum element size $l_{\max}$ should satisfy

$$l_{\max} \le \left(\frac{1}{8} \sim \frac{1}{5}\right) L \tag{2}$$

For a given finite element mesh, this rule equivalently puts an upper limit on the applicable dimensionless excitation frequency, a_0, on a specific mesh, i.e.

$$a_0 \le \left(\frac{1}{8} \sim \frac{1}{5}\right) \frac{2\pi b}{l_{\max}} \tag{3}$$

Finite element simulation of wave propagation requires an absorbing boundary along the finite domain to allow an effective transmission of the outgoing waves. The energy dissipation mechanism of transmitting waves outwards is referred as radiation damping. Viscous damping boundary (Lysmer and Kuhlemeyer, 1969) and infinite element boundary (Lynn and Hadid, 1981) are most widely used absorbing boundaries, both of which are available in the commercial software ABAQUS Version 6.4. However, either viscous damping boundary or infinite element boundary in ABAQUS results in unexpected numerical oscillations if the selected domain is not large enough.

To avoid the uncertainty of absorbing boundary, a reliable alternative is to set up a finite domain large enough to achieve steady state response before the wave reflection at boundary contaminates the dynamic response of foundation (Borja et. al., 1993). For this purpose, the scale of the finite domain needs to satisfy

$$nTv_p \le L_r \tag{4}$$

where L_r is the length of the shortest wave reflection path within the finite domain, v_p is the longitudinal wave velocity, T is the period of harmonic excitation, n is the number of periods from beginning including one full cycle of steady state response. Substituting

dimensionless frequency a_0 into Eq. (4) for period T yields the lower bound on the applicable dimensionless excitation frequency, a_0.

$$2n\pi \frac{b}{L_r} \cdot \sqrt{\frac{2-2\nu}{1-2\nu}} \le a_0 \tag{5}$$

A finite mesh of H=250m, D=250m, l_{max}=1.25m (refer to Fig. 2) was set up for a strip foundation of half-width b=1m on soil medium of v_s=201.5m/s, ν=0.25, ρ=1600kg/m^3. Eq. (5) gives lower bound of excitation frequency as $a_0 \ge 0.04$ while Eq. (3) gives upper bound of excitation frequency as $a_0 \le 1.0$. For input frequency within this range, the numerical oscillation is limited. The dynamic stiffness parameters computed by Finite element method using commercial software ABAQUS are plotted in Figure 3 against the analytical solution given by Hryniewicz (1981). The results show an excellent agreement, which validates the capacity of finite element method in modeling of the foundation-soil system.

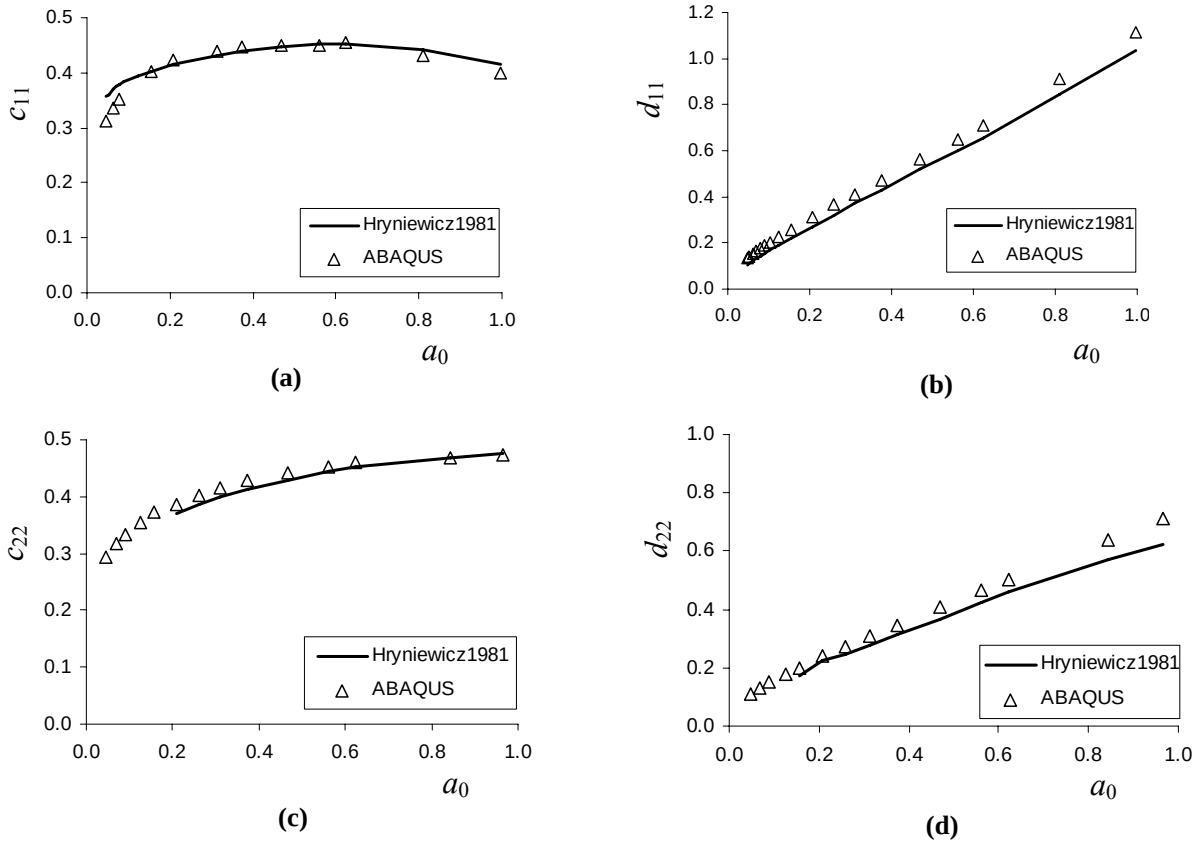

Fig. 3 Dynamic stiffness parameters from FEM model: (a)(b) vertical direction, (c)(d) horizontal direction

Further analyses show that the effect of either foundation half-width or Young's modulus of soil medium on dynamic stiffness parameters can be normalized by means of dimensionless frequency a_0 as shown in Figure 4 where the results of a foundation half-width b=1m and 2m (a and b) and different Young's modulus (c and d) are compared.

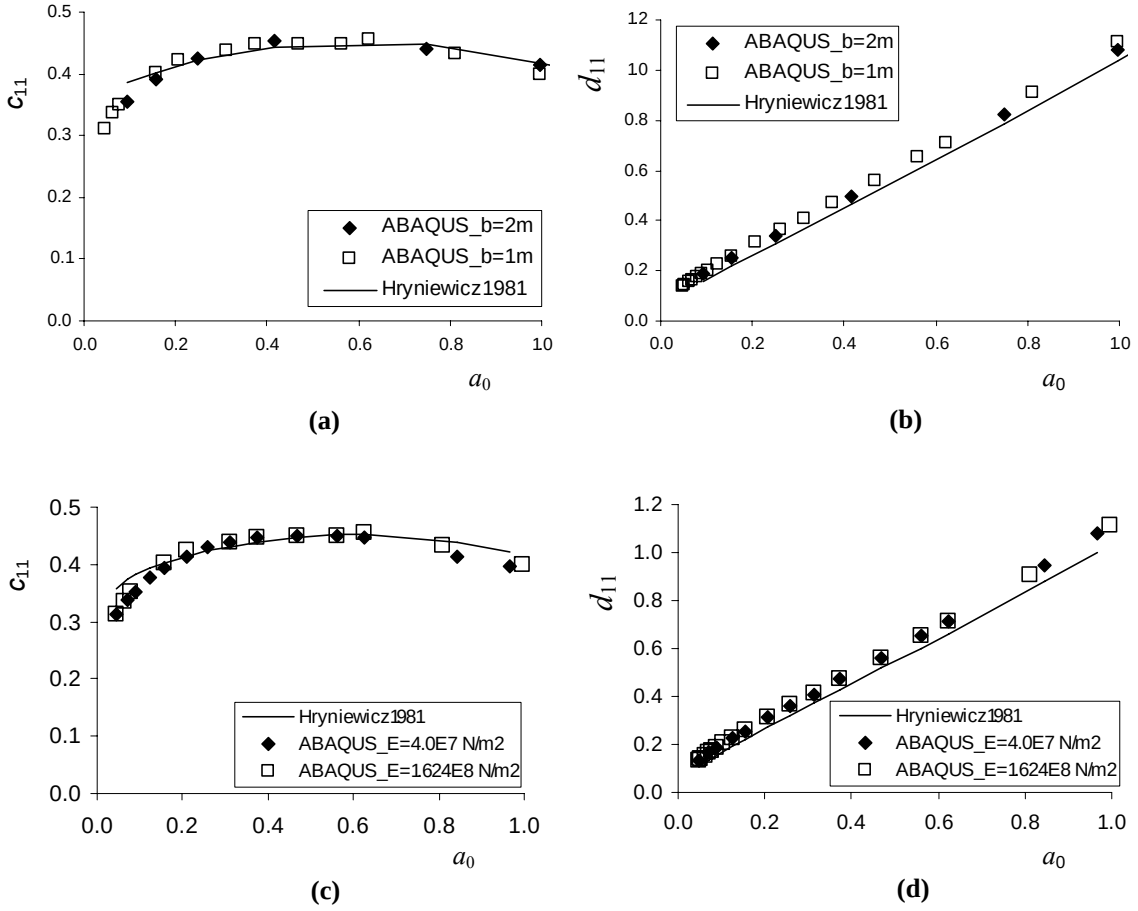

Fig. 4 Effect of foundation half-width and Young's modulus of soil

Another important property of elastic soil, the Poissson's ratio v, also affects the relationship between dimensionless dynamic stiffness parameters c_{11}, d_{11}, c_{22}, d_{22} and dimensionless frequency a_0 (Figure 5). The family of c_{11}–a_0 curves and d_{11}–a_0 curves corresponding to different Poisson's ratio describe completely the vertical dynamic stiffness of rigid strip foundation on elastic soil half-space (Figure 5 a and b). Similarly, c_{22} –a_0 curves and d_{22}– a_0 curves describe completely the horizontal dynamic stiffness (Figure 5 c and d). For practical use, the following simplified formulas are developed based on finite element analysis results:

$$c_{11} = \frac{a_0}{1.2a_0^3 - 1.1a_0^2 + 2.4a_0 + 0.04} + 0.55(\nu - 0.25) \tag{6}$$

$$d_{11} = 0.1 + (3.4\nu^2 - 0.5\nu + 0.9)a_0 \tag{7}$$

$$c_{22} = \frac{a_0}{0.45a_0^3 - 0.83a_0^2 + 2.46a_0 + 0.06} + \left[0.67(\nu - 0.25) + 0.01\right] \cdot (0.47a_0 + 0.56) \tag{8}$$

$$d_{22} = 0.1 + 0.65a_0 \tag{9}$$

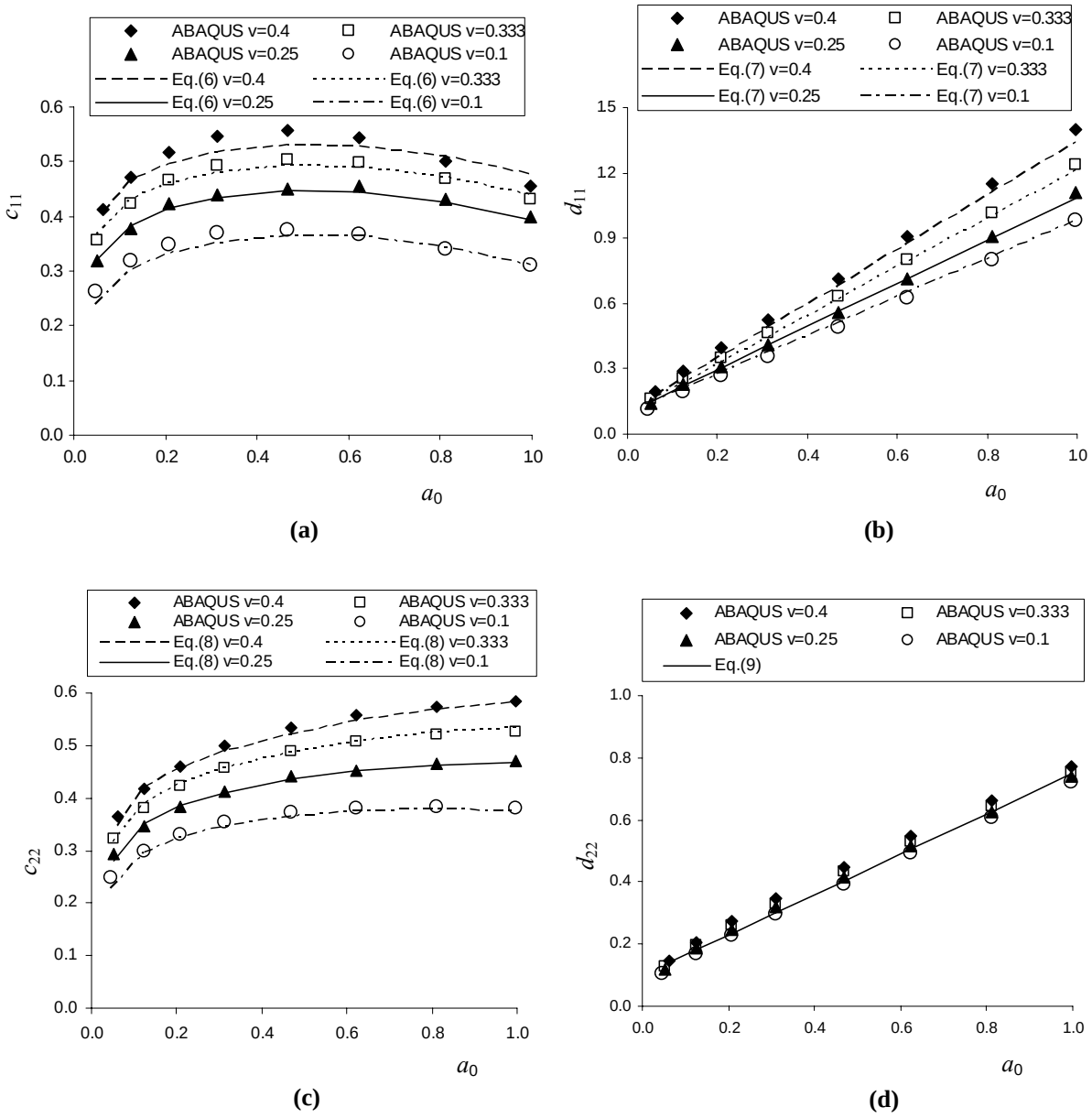

Fig. 5 Effect of Poisson's ratio of soil on dynamic stiffness along vertical (a and b) and horizontal direction (c and d)

The predicted c_{11} values with Eq. (6) and d_{11} values with Eq. (7) are compared with the finite element results in Figure 5 and showed excellent agreement. Similarly, the predicted c_{22} values with Eq. (8) and d_{22} values with Eq. (9) are also compared well with the finite element results in Figure 5 for horizontal direction. In computing the parameters c_{ii} and d_{ii} by finite element method, equations (10) to (12) are followed.

$$C(\omega) = \frac{W_d}{\pi\omega U_0^2} \tag{10}$$

$$d_{ii} = \frac{\omega \cdot C(\omega)}{\pi G} = \frac{a_0 \cdot C(\omega)}{\pi b\sqrt{G\rho}}, \quad i=1,2 \tag{11}$$

$$c_{ii} = \frac{P(t)/(\pi G U_0) - d_{ii}\cos(\omega t)}{\sin(\omega t)}, \quad i=1,2 \tag{12}$$

where $C(\omega)$ is equivalent dashpot value, W_d is the dissipated energy per loading cycle, U_0 is the displacement amplitude, $P(t)$ is the reaction force at time t.

Radiation Damping of Rigid Strip Foundation on Nonlinear Soil Medium

During strong earthquakes, soil often behaves nonlinearly. The plasticity experienced in soil reduces the energy dissipated through outgoing waves. As result, radiation damping of nonlinear soil is quite different from that of linear soil. Analytical derivation meets big difficulty to deal with the dynamic response of shallow foundation on nonlinear soil half-space. Alternatively, finite element modeling is an effective way to reveal the amplitude and frequency dependent nature of the foundation-nonlinear soil system.

In this section, the finite element method is used to evaluate the radiation damping of rigid strip foundation on nonlinear soil medium. It is recognized that the response of an infinitely long strip foundation sitting on nonlinear soil medium behaves differently under static cyclic loading and dynamic harmonic excitation, as shown in Figure 6. The area within static loop accounts for hysteretic energy W_h only and is frequency independent. On the other hand, the area within dynamic loop accounts for total dissipated energy W_t through both hysteretic and radiation damping, which depends on excitation frequency. The difference between W_t and W_h is therefore the nonlinear radiation energy, W_d, which is related to nonlinear radiation dashpot coefficient C in Eq. (10) and nonlinear radiation damping parameter d in Eq. (11).

A simple procedure has been developed to derive the model parameters for nonlinear constitutive model of soil based on widely available shear modulus reduction curves. Stress-strain relationship for simple shear can be easily obtained from shear

modulus reduction curves. By applying the Masing rule to this 1D stress-strain relationship, one can obtain a cyclic loop, similar to the one shown by continuous line in Figure 7, where the soil parameters associated with Painter Street Bridge (Zhang and Makris 2002) are used. The Bouc-Wen model (Wen 1976) is then used to simulate the cyclic loop as shown by the dashed line in Figure 7. Excellent agreement can be obtained easily by adjusting the model parameters of Bouc-Wen model. This procedure allows for easy generation of cyclic behavior of different soil types so that the effects of various soil properties such as initial stiffness, yield stress and post-yielding stiffness can be evaluated.

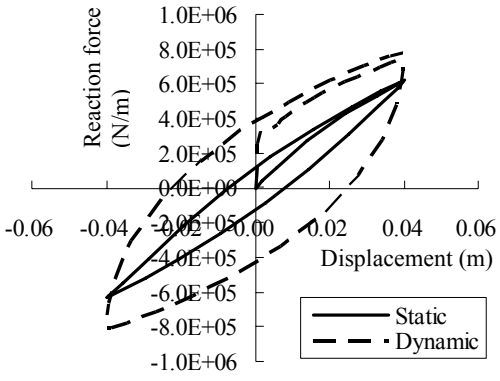

Fig. 6 Static response and dynamic response of nonlinear soil

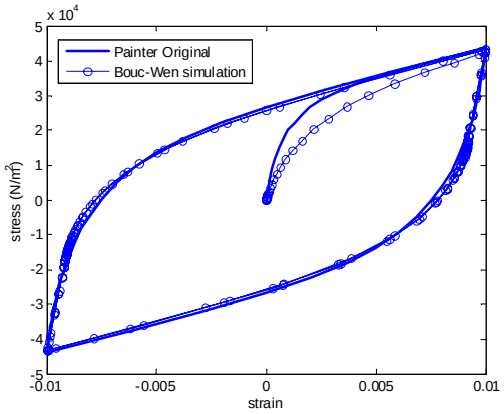

Fig. 7 Bouc-Wen model for simple shear

An elasto-plastic material model of Von-Mises yield criterion and nonlinear kinematic hardening rule in ABAQUS was chosen to model nonlinear soil behavior. The elasto-plastic material model was defined by a few representative points on the steady-state cyclic loop, e.g. the one given by Bouc-Wen model in Figure 7. Figure 8 compares the response of a single plane-strain element subjected to simple shear predicted by ABAQUS and the input curve based on Masing rule. The input to ABAQUS was done by picking up four representative points from the Bouc-Wen loop in Figure 7 and the program computes the nonlinear kinematic hardening parameters automatically. The excellent agreement shown on Figure 8 verifies this procedure.

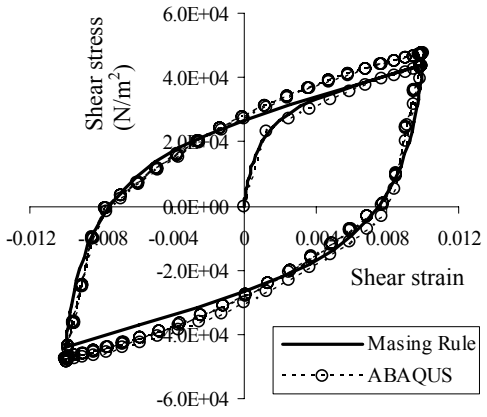

Fig. 8 ABAQUS simulation of simple shear

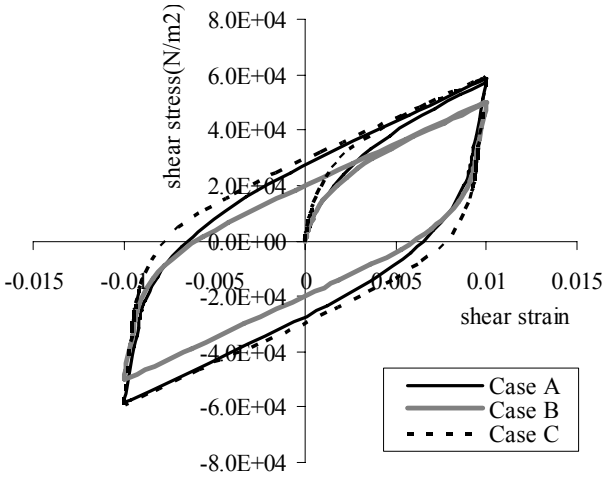

Fig. 9 ABAQUS simulation of simple shear

Parametric studies are performed on three distinct pairs of soil models to evaluate the effects of initial stiffness, yielding stress and post yielding stiffness on dynamic stiffness of the strip foundation on nonlinear soil medium. Three Bouc-Wen simple shear loops, Case A, B and C, were generated for this purpose (Fig. 9). Case A differs from Case B only in yield shear stress τ_y, which is $3.0\text{x}10^4$ N/m^2 and $2.1\text{x}10^4$ N/m^2 for Case A and B respectively. Case A differs from Case C only in shear modulus G, which is $6.0\text{x}10^7$ N/m^2 and $1.0\text{x}10^8$ N/m^2 for Case A and C respectively. Poisson's ratio 0.25 is specified for all three soil material cases.

Besides Eq. (3) and Eq. (5), the possible development of plasticity in soil medium should also be taken into account to set up finite element mesh for nonlinear dynamic analysis. Development of plasticity results in smaller wave velocity, which requires finer mesh in the region where soil yields. Following all the restrictions and taking advantage of symmetry or anti-symmetry, two plane strain finite element meshes was set up for different excitation frequency ranges. For frequency range 0.4Hz~1.0Hz, the mesh is of H=D=1800m, l_{max}=10m and has uniform finer rectangular elements of 0.1mx0.1m within the 12mx12m region near the foundation. For frequency range 1.0Hz~3.0Hz, the mesh is of H=D=700m, l_{max}=3m and has uniform finer rectangular elements of 0.1mx0.1m within the 14mx14m region near the foundation.

Effect of soil density is discussed at first. Dynamic finite element analyses of a strip foundation of half-width b=1m on soil medium of material Case A under vertical harmonic excitation $U(t) = 0.02\sin\omega t$ (meter) were performed with different soil densities ρ=800kg/m^3, 1600kg/m^3, 2000kg/m^3 respectively. Figure 10 plots d_{11} vs. a_0 curves for different soil density. It shows that soil density does not affect the dimensionless nonlinear radiation damping parameter.

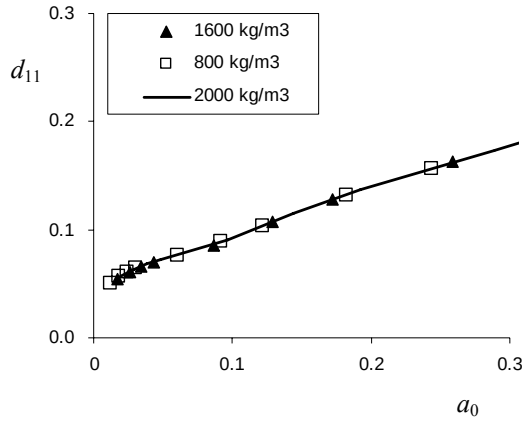

Fig. 10 Effect of soil density

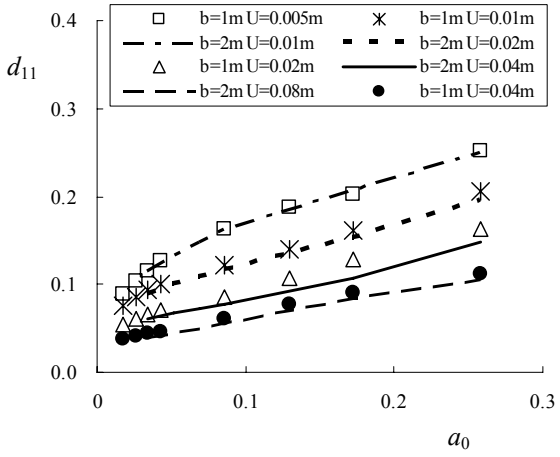

Fig. 11 Effect of ratio U_0/b

It is anticipated that the amplitude of displacement excitation will affect the development of nonlinearity in soil medium. As a result, nonlinear radiation damping is

displacement-amplitude dependent, as differs from linear radiation damping. Figure 11 plots the nonlinear radiation damping for soil material Case A with density of ρ=1600kg/m^3 and different combinations of foundation half-width b and displacement amplitude U_0. It is observed from Figure 11 that the nonlinear radiation damping parameter depends on the ratio U_0/b rather than U_0 itself. Analyses with soil material Cases B and C gave the same conclusion. Larger U_0/b results in more nonlinearity in soil, which leads to smaller radiation damping due to outgoing waves.

Besides the ratio U_0/b, soil properties affect the nonlinear behavior of strip foundation. Figure 12 shows the static responses of a strip foundation of b=2m under vertical cyclic displacement of amplitude 0.04m with soil material Case A, B, C respectively. Case A and Case B lead to different yield displacement in foundation behavior. Case A and Case C lead to different initial stiffness in foundation behavior.

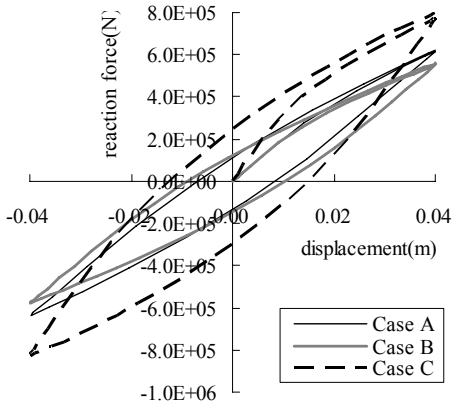

Fig. 12 Static cyclic behavior of foundation

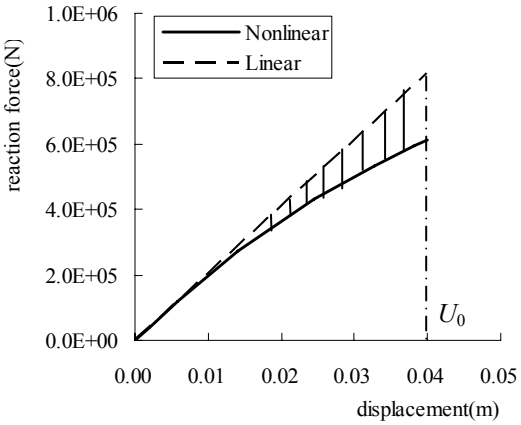

Fig. 13 Static behavior of foundation

Static analysis of the strip foundation on nonlinear soil with finite element method gave a nonlinear initial loading curve as shown in Figure 13. Assuming small deformation, the initial linear portion of the nonlinear curve can be extended to any displacement level to get the linear counterpart. The deviation of the nonlinear curve from its linear counterpart indicates the degree of nonlinearity in the soil medium. To quantify the degree of nonlinearity in soil medium under displacement excitation at foundation, nonlinearity indicator δ is defined as

$$\delta = \frac{W_{linear} - W_{nonlinear}}{W_{linear}} \tag{13}$$

where W_{linear} is the work done along linear loading path from the origin to U_0, $W_{\text{nonlinear}}$ is the work done along nonlinear loading path from origin to U_0. The shaded area in Fig.13 illustrates the numerator in Eq. (13). Essentially, the nonlinear indicator covers both the effect of U_0/b and the effect of nonlinear soil properties at a global level.

Static finite element analyses were performed to get nonlinearity indicators for the combinations of different soil material cases and U_0/b ratios as listed in Table 1. Larger nonlinearity indicator indicates more nonlinearity in soil. Nonlinear dynamic analyses with finite element method gave nonlinear radiation damping parameters of the combinations of different soil material cases and U_0/b ratios as plotted in Figure 14. Referring to Table 1, Figure 14 reveals that the radiation damping decreases monotonically with development of nonlinearity in soil medium i.e. increase of nonlinearity indicator. The results show the great promise of using the nonlinearity indicator as quantifying parameter for radiation damping of strip foundation on nonlinear soil medium.

Table 1. Nonlinearity indicators for different combinations

	U_0/b=0.005	U_0/b=0.01	U_0/b=0.02
Soil Case A	4.37E-03	3.95E-02	1.54E-01
Soil Case B	1.08E-02	8.32E-02	2.16E-01
Soil Case C	3.11E-02	1.49E-01	3.16E-01

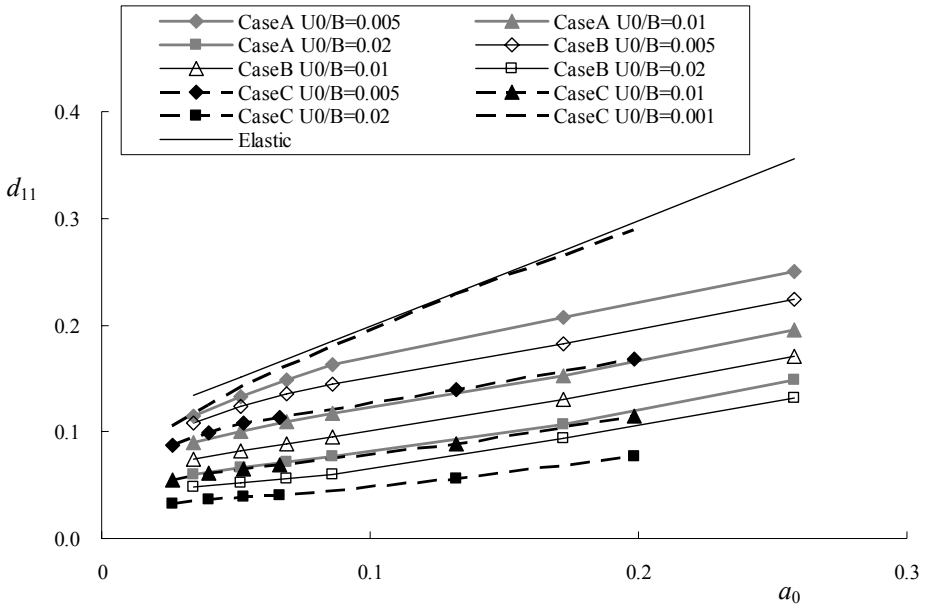

Fig. 14 Nonlinear radiation damping

Conclusion

In this study, the dynamic stiffness of strip foundation on linear and nonlinear soil medium is analyzed by finite element method. The numerical results are compared with the theoretical solution of strip foundations resting on elastic half-space. Special attentions are paid to choosing appropriate domain scale, mesh size and boundary

conditions so that the wave propagation in an infinite domain can be correctly modeled. Excellent agreement between finite element analysis and theoretical results can be achieved by judicious selection of domain scale and mesh size. Closed-form formulas are then developed to describe the spring and dashpot constants of dynamic stiffness as function of frequency as well as their dependency on foundation width, Young's modulus and Poisson's ratio. The analysis of strip foundation on nonlinear soil medium shows that energy dissipation depends on the amplitude of the motion and frequency. The plasticity in soil reduces the energy dissipated through outgoing waves. As result, the radiation damping of nonlinear soil is significantly lower than the elastic soil counterpart. The study investigated the effects of initial elastic stiffness, yielding stress and post-yielding stiffness on radiation damping. A nonlinearity indicator is developed and has been shown to directly relate to the reduction of radiation damping due to soil yielding. The findings are important to dynamic responses of bridges supported on shallow foundations since the reduced radiation damping at foundation level will result in increased structural response.

Acknowledgement

Partial financial support for this study was provided by National Science Foundation under grant NEESR-0421577.

References

Borja, R. I., Wu, W-H. and Smith, H.A. (1993), "Nonlinear response of vertically oscillating rigid foundations", *Journal of Geotechnical Engineering*, ASCE, 119 (5):893-911.

Gazetas, G. (1991), "Formulas and charts for impedances of surface and embedded foundations", *Journal of Geotechnical Engineering*, 117(9):1361-1381.

Hryniewicz Z. (1981), "Dynamic response of a rigid strip on an elastic half-space", *Computer Methods in Applied and Mechanical Engineering*, 25:355-364.

Kuhlemeyer, R.L. and Lysmer, J. (1973), "Finite element method accuracy for wave propagation problems", *Journal of Soil Mechanics and Foundations Division*, ASCE, 99(SM5):421-427.

Luco, J.E. and Westmann, R.A. (1972), "Dynamic response of a rigid footing bonded to an elastic half space", *Journal of Applied Mechanics*, ASME, 39(2):527–534.

Lysmer, J. and Kuhlemeyer, R.L. (1969), "Finite dynamic model for infinite media", *J. Engrg. Mech. Div.*, ASCE, 95(4):859-877.

Lynn, P.P. and Hadid, H.A. (1981), "Infinite elements with 1/rn type decay", *International Journal for Numerical Methods in Engineering*, 17(3):347-355.

Muskhelishvili, N. I. (1963), "Some Basic Problems of the Mathematical Theory of Elasticity", P. Noordhoff, Gröningen, the Netherlands.

Veletsos, A.S. and Verbic, B. (1974), "Basic response functions for elastic foundations", *Journal of Engineering Mechanics*, 100(EM2):189-202.

Veletsos, A.S., Prasad, S.M., and Wu, W.H. (1997), "Transfer functions for rigid rectangular foundations", *Journal of Earthquake Engineering and Structural Dynamics*, 26(1):5-17.

Wen, Y-K. (1976), "Method for random vibration of hysteretic systems", *Journal of Engineering Mechanics Division*, ASCE, 102(EM2):249-263.

Zhang J. and Makris N. (2002), "Kinematic response functions and dynamic stiffnesses of bridge embankments", *Earthquake Enginnering and Structural Dynamics*, 31(11):1933–1966.